UNIVERSITY OF COPENHAGEN

Imaging electromigration during the formation of break junctions.

Taychatanapat, Thiti; Bolotin, Kirill I; Kuemmeth, Ferdinand; Ralph, Daniel C

Imaging Electromigration during the Formation of Break Junctions

Thiti Taychatanapat, Kirill I. Bolotin, Ferdinand Kuemmeth, and Daniel C. Ralph*

*Laboratory of Atomic and Solid State Physics, Cornell University,
Ithaca, New York 14853*

Ⓦ **This paper contains enhanced objects available on the Internet at http://pubs.acs.org/nano.**

ABSTRACT

Using a scanning electron microscope, we make real-time movies of gold nanowires during the process of electromigration. We confirm the importance of using a small series resistance when employing electromigration to make controlled nanometer-scale gaps suitable for molecular-electronics studies. We are also able to estimate the effective temperature experienced by molecular adsorbates on the nanowire during the electromigration process.

Breaking metal wires by electromigration has proven to be a useful technique for making nanometer-scale gaps between metal electrodes into which individual molecules can be inserted to measure their electrical properties.[1−4] However, there remains considerable uncertainty about some aspects of the electromigration process. Some research groups have found that a high percentage of gaps formed during electromigration (10−30%) can contain metal nanoparticles that produce artifacts in the device's electrical characteristics (Coulomb blockade and the Kondo effect) that might be mistaken for molecular signals.[5−7] Other groups, using slightly different procedures for electromigration, observe these artifacts at much lower rates.[2,8,9] In addition, the degree to which metal wires become heated during the electromigration process is not well understood. This is an important issue because the molecules used for making single-molecule electrical devices are often attached to the device before electromigration is performed, and high temperatures might damage or destroy some molecules. Here, we investigate these issues by observing the electromigration process in real time within a scanning electron microscope. We provide direct confirmation for arguments[5,10,11] that the amount of series resistance in the electromigration circuit is a critical parameter in controlling the overall morphology of the junction after electromigration and whether nanoparticles are formed within the device. By observing devices to which metal nanoparticles have been attached before electromigration using linker molecules, we are also able to estimate the effective temperature experienced by molecular adsorbates.

We examine electromigration in gold wires formed on top of an oxidized aluminum layer. This Al layer is designed
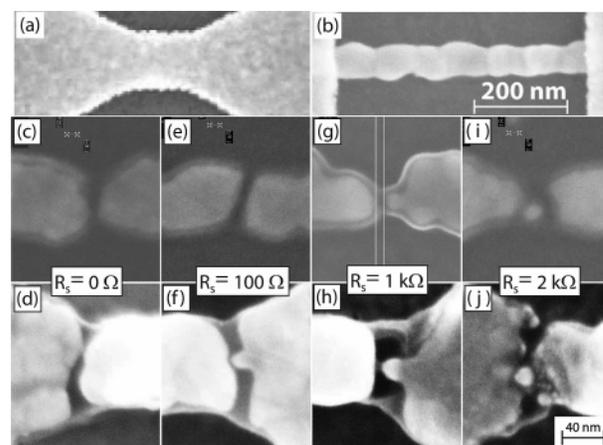

Figure 1. (a,b) Scanning electron microscopy (SEM) images of a bow-tie sample and long-wire sample before electromigration. The 200 nm scale bar in (b) also applies to (a). (d−j) SEM images of gaps formed by electromigration. The middle row of images shows long-wire samples, and the bottom row shows bow-tie samples. The external series resistance, R_s, connected to the wires is (c,d) $R_s = 0\ \Omega$, (e,f) $R_s = 100\ \Omega$, (g,h) $R_s = 1\ k\Omega$, and (i,j) $R_s = 2\ k\Omega$. The 40 nm scale bar applies in (c−j).

for use as a gate electrode in future studies; during our experiment, it is not connected so that its electrical potential is left floating. The device fabrication begins with the use of photolithography to define a 2.8 μm wide 16 nm thick Al film with 2 nm of Ti as a sticking layer on an oxidized Si substrate. This deposition is conducted at liquid nitrogen temperature to enhance the smoothness of the Al layer, after which the samples are warmed overnight to room temperature in 50 mTorr of O_2 and then exposed to air. The Au wires are fabricated with electron-beam lithography, evaporation

of Au onto the substrates while they are at room temperature (with no sticking layer), and liftoff. We investigated two different shapes of gold wires: "bow-tie" samples (Figure 1a) 23 nm thick with a minimum width of $100-150$ nm, and longer straight wires (Figure 1b) 20 nm thick, 550 or 740 nm long, with an average width of $65-100$ nm. The edges of the straight wires are not smooth because we do not use a sticking layer for the Au deposition, and therefore the grain size can be comparable to the width of the wire. The wires are connected to gold contacts (2 μm wide and 23 nm thick for bow-tie samples, and 3 μm wide and 40 nm thick for straight wires). The as-fabricated two-probe resistances (including contact pads) are $50-120$ Ω. Just before beginning the electromigration, we clean each chip in an oxygen plasma for 2 min.

We conduct electromigration studies at room temperature in the ultrahigh vacuum (UHV) chamber of a LEO 1550 scanning electron microscope (SEM). The UHV conditions minimize carbon contamination on the samples during imaging, which might otherwise affect the electromigration process. Electrical feedthroughs installed in the chamber enable us to control the applied bias voltage and measure the current during the breaking process. Thirteen samples can be contacted simultaneously on each chip. For studies as a function of the series resistance, we add discrete resistors to our circuit outside the microscope. The primary results of our studies are movies showing how the samples evolve during the course of electromigration. The SEM is capable of recording $2-10$ images per s depending on the scan size and speed.

We first discuss electromigration performed by applying a simple voltage ramp with no added series resistance in the biasing circuit. This is the process that our group uses most commonly for making single-molecule devices. Ⓦ Movie 01a (in MPEG format) shows this process for a straight-wire sample and Ⓦ Movie 01b (in MPEG format) for a bow-tie sample, both in real-time speed. The voltage is ramped at a rate of 10 mV/s for the straight-wire sample and a rate of 30 mV/s for the bow-tie sample. For the straight-wire sample, electromigration starts at $\sim$0.28 V, and the wire is completely broken at $\sim$0.30 V. For the bow-tie sample, electromigration begins at $\sim$0.47 V and is complete at $\sim$0.54 V. In general, we find that the two types of wires break at different average applied voltages (in the range $0.3-0.4$ V for the straight wires and $0.5-0.6$ V for the bow-tie samples in the absence of any added external series resistance), but we do not observe any clear qualitative differences in the processes by which they break. Throughout the electromigration process for these wires and 18 other similar samples, the morphology of the wire always changed gradually, without the formation of any visible nanoparticles that were separate from the main wire. For this reason, we expect that a large majority of our wires broken under these bias conditions will form simple tunnel junctions, without nanoparticles in the junction region that may cause transport artifacts.

Ⓦ In Ⓦ Movie 02a (in MPEG format) and Ⓦ Movie 02b (in MPEG format), we perform electromigration using active feedback to control the bias voltage, following Strachan et al.[12] With no added series resistance in the biasing circuit, we ramp the voltage at a rate of 10 mV/s until the DC resistance of the wire reaches a setpoint value. Then, the voltage is decreased abruptly by 10%, the setpoint resistance is incremented by 2%, and the voltage ramp is reinitiated. This process repeats until the sample reaches the desired final resistance. In Movie 02a, we observe the start of electromigration near $\sim$0.21 V as a loss of gold near one of the grain boundaries in the wire. As electromigration proceeds, the narrowest region of the wire gradually shifts and the geometry of the contact can evolve considerably, so that the direction of electron flow in the constriction can vary by as much as 90°. The length of the movie corresponds to 56 s in real time. The final breaking of this wire was not recorded. Movie 02b corresponds to 67 s in real time. Other than the much slower speed with which the breaking proceeds, we see few differences in the final results of electromigration conducted with and without active feedback.

Several groups have noted that if the biasing circuit for electromigration includes significant series resistance (e.g., due to resistive wiring in a low-temperature cryostat), then the breaking process can be altered dramatically.[5,10,11] Initially, much of the applied voltage will drop across the series resistance. However, as electromigration proceeds and the resistance of the contact grows relative to the series resistance, a greater fraction of the applied voltage will fall across the contact and the electromigration process can be accelerated. If the series resistance is sufficiently large relative to the contact resistance, this can lead to an instability in which the electromigration process runs away and the breaking occurs with a much larger voltage across the contact than would be the case in the absence of series resistance. Our movies demonstrate that the result can be a violent, explosive rupture of the wire. Ⓦ Movie 03 (in MPEG format) shows, in real-time speed with $\sim$1.3 images per s, a straight gold wire electromigrated using a simple voltage ramp (30 mV/s) applied to the combination of the sample resistance and 1 kΩ of added series resistance. The start of electromigration becomes visible first at $\sim$3.8 V, and there is a short period of gradual change in the contact, but then the wire breaks suddenly (or explodes) at $\sim$4.0 V. If we continue to increase the voltage even after this first break, we observe that additional changes in the contact region are still possible; the wire breaks violently again, and gold in the junction region can move under the influence of the applied bias to reform a contact. Similar processes have been inferred previously in studies of mound formation by scanning tunneling microscopes[13] and in the formation of bridges of Au across 70 nm slits.[14]

In Ⓦ Movie 04 (in MPEG format), a bow-tie Au wire is connected to 2 kΩ series resistance, and active feedback with a sweeping rate of 10 mV/s is used to break the wire. The movie plays in real-time speed. The formation of a gap in the wire starts slowly at $\sim$7.94 V, but the wire suddenly explodes at $\sim$8.12 V. The failure of the wire occurs more quickly than our active feedback can respond ($\sim$30$-$100 ms) to decrease the bias voltage.
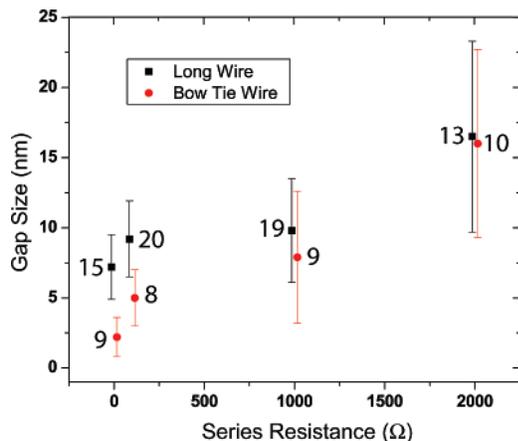
Figure 2. The average width of gaps formed by electromigration of gold wires at room temperature as a function of added external series resistance. Error bars denote standard deviations. The gap sizes are estimated from SEM images. The number of samples included in each average is shown next to the graphed points.

For both the bow-tie and straight-wire configurations, we have imaged how the final configuration of the junctions after breaking depends on the amount of series resistance, using trials with zero added series resistance and 100 Ω, 1 kΩ, and 2 kΩ series resistance. In this study, we performed electromigration using simple voltage ramps at 30 mV/s at room temperature in air, until the resistance of each sample was ≳ 10^6 Ω. Representative images of the broken wires are shown in Figure 1c−j, and the gap sizes measured by SEM averaged over many samples are shown in Figure 2. The average gap width increases significantly with added series resistance, particularly for the 2 kΩ tests. Even with zero added series resistance, the gap sizes measured at room temperature are larger than the gaps inferred from tunneling resistances measured in wires electromigrated at cryogenic temperatures. These increased gap sizes for samples with low series resistance may be due to relaxation of the gold electrodes at room temperature after the electromigration process is finished, rather than being a direct result of difference in the electromigration process between 4.2 K and room temperature.[9] The morphology of the junction also depends on the series resistance. Gold nanoparticles in the gap region, separate from the main electrodes, were observed in 3 out of 10 bow-tie samples with 2 kΩ series resistance, and 5 out of 13 straight-wire samples with 2 kΩ series resistance, but not in any of the samples with lower series resistance.

We now turn to the question of what is the extent of heating in the case of the more controlled, gradual electromigration process performed without added series resistance. The effective *electronic* temperature in biased metal contacts has been analyzed previously in some simple limits. In the case of fully diffusive electron transport, when the inelastic mean free path for electron scattering is less than the contact radius and heat flow away from the junction is dominated by electron transport governed by the
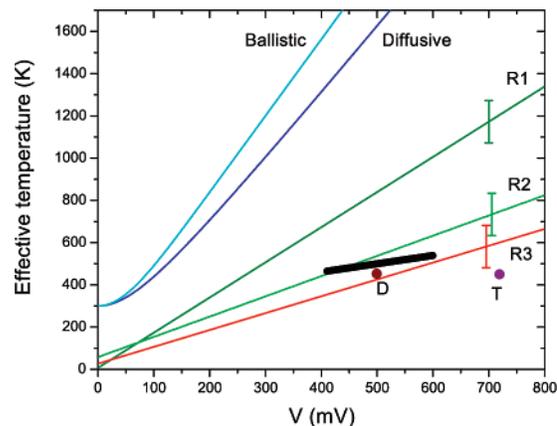

Figure 3. Different estimates of heating in metal contacts. The thick black line shows our estimate, determined as discussed in the text. The lines R1, R2, and R3 are linear extrapolations from the data of Ralls et al.[19] for Al, Pd, and Cu contacts, respectively, measured at $V < 120$ mV at low temperature. The points D and T denote values reported by Durkan et al. (453 K at $V = 0.5$ V)[21] and Trouwborst et al. (450 K at $V = 0.72$ V).[11] The curves labeled "Diffusive" and "Ballistic" show the effective-electron-temperature estimates of eqs 1 and 2 with $T_0 = 300$ K.

Wiedemann−Franz Law, the maximum electron temperature $T_{el,diffusive}$ in the middle of the contact is[15]

$$T_{el,diffusive}^2 = T_0^2 + \frac{3}{4}\left(\frac{eV}{\pi k_B}\right)^2 \tag{1}$$

where T_0 is the background temperature and k_B is the Boltzmann constant. In the opposite limit of a ballistic contact, with a contact radius less than the electron mean free path, the electron distribution is nonthermal. However, an effective electronic temperature can still be assigned by imagining that a stationary harmonic oscillator is coupled to the electrons via inelastic scattering and then calculating the degree of excitation for this oscillator. The resulting occupation of harmonic-oscillator levels is described by a thermal distribution, with[16]

$$T_{el,ballistic} = \frac{3}{8}T_0 + \frac{5}{16}\frac{eV}{k_B}\coth\left(\frac{eV}{2k_B T_0}\right) \tag{2}$$

The expressions for $T_{el,diffusive}$ and $T_{el,ballistic}$ are plotted in Figure 3. These estimates for T_{el} can grow to be very large during electromigration; for $V = 0.5$ V across a contact, both estimates suggest $T_{el} > 1625$ K, much greater even than the melting point of gold (1337 K). However, the effective temperature governing ionic motion in electromigration is expected to be much lower, both because the ions will interact with cooler phonon modes as well as with electrons[17] and because phonons are traveling waves so they will not be heated to the same degree as a stationary harmonic oscillator imagined to be at the center of a contact.[17,18] The degree of heating associated with ionic dynamics has been measured directly for $V < 120$ mV in metal nanocontacts by tracking the switching rates of individual defects as they move between two different configurations, producing two-

level resistance fluctuations as a function of time.[19,20] In the regime $eV \gg k_B T$, the dependence of the measured effective temperatures T_{ion} are to good accuracy linear in V, with a measured amount of heating 2−5 times lower than the predicted rise in electron temperature. Linear extrapolations to $V > 120$ mV of effective temperatures measured by Ralls et al.[19] are shown in Figure 3. Average effective temperatures during electromigration in Au have also been estimated based on the change in contact resistance at high bias.[11,21,22] These studies found T_{eff} in the range 450−525 K for breaking voltages 0.5−0.72 V.

We can gain more direct insight into the effective temperature experienced by molecular absorbates during electromigration by imaging the breaking of wires with gold nanoparticles attached on top. We assembled the nanoparticles onto our Au wires using a protocol adapted from Liu et al.[23] A chip with unbroken Au wires was first cleaned in oxygen plasma and then immersed in 3-(2-aminoethylamino)propyl]trimethoxysilane (APTS, $(CH_3O)_3Si(CH_2)_3NH-(CH_2)_2NH_2)$[24] for 10 min to form a self-assembled monolayer. After rinsing with deionized water, we baked the chip at 120 °C for 30 min and then immersed it overnight in a solution with equal volumes of 0.026 M citric acid and a solution of 15 nm Au colloid particles with 1.4×10^{12} particles per mL. Finally, the chip was rinsed in deionized water and dried.

Ⓦ Movie 05 (in MPEG format) shows, in real-time speed, the electromigration process for this type of sample, for a simple voltage ramp with no added series resistance. The direction of electron flow is from right to left. When the voltage reaches ∼0.41 V, the Au nanoparticles located on top of the nanowire begin to disappear one by one. By the time that electromigration of the underlying wire is first visible (at $V \sim 0.55$ V), almost no particles remain near the gap region. In contrast to the nanoparticles attached on top of the gold nanowire, particles located immediately adjacent to the edges of the Au wire, on top of the Al gate electrode, are not perturbed during the electromigration. The wire breaks completely at ∼0.6 V. We find quite generally for the bow-tie samples that the final break occurs at the negative-polarity end of the nanowire (the electron source) and not at the middle.

Most likely, the nanoparticles that disappear in Movie 05 do not simply melt. Either their gold atoms diffuse through the APTS monolayer to the electrode at sufficiently high temperatures, or temperature-induced fluctuations of the molecular monolayer may allow the nanoparticle to contact the gold electrode, at which point surface diffusion of gold atoms would cause the nanoparticle to be absorbed into the electrode. By comparing to the results of thermal annealing for identically prepared test samples, we can estimate the effective temperature of the adsorbed nanoparticles. We annealed test samples at 390, 440, and 490 K for 30 min. The attached nanoparticles survive at 390 and 440 K, but disappear completely by 490 K. We can therefore conclude that the effective temperature influencing the adsorbed nanoparticles is greater than 440 K when the nanoparticles begin to disappear at $V = 0.41$ V (Figure 3). Extrapolating

to higher V by assuming that the amount of heating above room temperature is proportional to the functional form of heating in either the diffusive or the ballistic predictions, we then estimate that the effective temperature at $V = 0.6$ V where electromigration is complete is $\gtrsim$515 K. At this temperature, some molecules used for molecular electronics should not be affected (e.g., fullerenes), but other molecules of potential interest (e.g., Mn_{12}(acetate)) would likely be damaged or destroyed.[25,26]

We have investigated whether an additional chemical treatment can better protect adsorbed nanoparticles during electromigration. We assembled bare Au nanoparticles onto an APTS monolayer as before and then immersed the chip in a 5 mM solution of dodecanethiol ($HSC_{12}H_{25}$) in ethanol for 24 h to encapsulate and charge-neutralize the nanoparticles.[23] Ⓦ Movie 06 (in MPEG format) shows the result of electromigration performed by applying a simple voltage ramp (30 mV/s) at real-time speed. We observe that many of the nanoparticles still disappear in the course of electromigration (with the first nanoparticles disappearing at 0.44 V), but others survive and can sometimes bridge the gap that results when the wire is broken. We suspect that the binding of dodecanethiol ligands to the nanoparticles helps to inhibit the diffusion of the nanoparticles through the APTS monolayer. Similar protocols for electromigration in the presence of metal nanoparticles might be developed into a way to make nanoparticle-based single-electron transistors in vacuum, a procedure that would be particularly useful for electrode materials (e.g., ferromagnets) whose surfaces are sensitive to air exposure.

In summary, we have observed the process of electromigration of Au wires in real time within a scanning electron microscope. In order to break the wires with simple, nanometer-scale gaps that are of interest for molecular-electronics studies, it is important to minimize the series resistance in the electromigration circuit. We estimate that the effective temperature affecting molecular absorbates during electromigration can be $\gtrsim$515 K.

References

(1) Park, H.; Lim, A. K. L.; Alivisatos, A. P.; Park, J.; McEuen, P. L. *Appl. Phys. Lett.* **1999**, *75*, 301.
(2) Park, J.; Pasupathy, A. N.; Goldsmith, J. I.; Chang, C.; Yaish, Y.; Petta, J. R.; Rinkoski, M.; Sethana, J. P.; Abruna, H. D.; McEuen, P. L.; Ralph, D. C. *Nature* **2002**, *417*, 722.
(3) Liang, W. J.; Shores, M. P.; Bockrath, M.; Long, J. R.; Park, H. *Nature* **2002**, *417*, 725.
(4) Yu, L. H.; Natelson, D. *Nano Lett.* **2004**, *4*, 79.
(5) Sordan, R.; Balasubramanian, K.; Burghard, M.; Kern, K. *Appl. Phys. Lett.* **2005**, *87*, 013106.
(6) Houck, A. A.; Labaziewicz, J.; Chan, E. K.; Folk, J. A.; Chuang, I. L. *Nano Lett.* **2005**, *5*, 1685.
(7) Heersche, H. B.; de Groot, Z.; Folk, J. A.; Kouwenhoven, L. P.; van der Zant, H. S. J. *Phys. Rev. Lett.* **2006**, *96*, 017205.

(8) Natelson, D.; Yu, L. H.; Ciszek, J. W.; Keane, Z. K.; Tour, J. M. *Chem. Phys.* **2006**, *324*, 267.

(9) Strachan, D. R.; Smith, D. E.; Smith, D. E.; Fischbein, M. D.; Johnston, D. E.; Guiton, B. S.; Drndic, M.; Bonnell, D. A.; Johnson, A. T., Jr. *Nano Lett.* **2006**, *6*, 441.

(10) Esen, M.; Fuhrer, M. S. *Appl. Phys. Lett.* **2005**, *87*, 263101.

(11) Trouwborst, M. L.; van der Molen, S. J.; van Wees, B. J. *J. Appl. Phys.* **2006**, *99*, 114316.

(12) Strachan, D. R.; Smith, D. E.; Park, T. H.; Therien, M. J.; Bonnell, D. A.; Johnson, A. T. *Appl. Phys. Lett.* **2005**, *86*, 043109.

(13) Mamin, H. J.; Guenthner, P. H.; Rugar, D. *Phys. Rev. Lett.* **1990**, *65*, 2418.

(14) Anaya, A.; Korotkov, A. L.; Bowman, M.; Waddell, J.; Davidovic, D. *J. Appl. Phys.* **2003**, *93*, 3501.

(15) Holm, R. *Electric Contacts*, 4th ed.; Springer-Verlag: Berlin, 1967.

(16) Chen, Z.; Sorbello, R. S. *Phys. Rev. B* **1993**, *47*, 13527.

(17) Kozub, V. I.; Rudin, A. M. *Phys. Rev. B* **1993**, *47*, 13737.

(18) Todorov, T. N. *Philos. Mag. B* **1998**, *77*, 965.

(19) Ralls, K. S.; Ralph, D. C.; Buhrman, R. A. *Phys. Rev. B* **1989**, *40*, 11561.

(20) Holweg, P. A. M.; Caro, J.; Verbruggen, A. H.; Radelaar, S. *Phys. Rev. B* **1992**, *45*, 9311.

(21) Durkan, C.; Welland, M. E. *Ultramicroscopy* **2000**, *82*, 125.

(22) Lambert, M. F.; Goffman, M. F.; Bourgoin, J. P.; Hesto, P. *Nanotechnology* **2003**, *14*, 772.

(23) Liu, S.; Zhu, T.; Hu, R.; Liu, Z. *Phys. Chem. Chem. Phys.* **2002**, *4*, 6059.

(24) Purchased from Sigma-Aldrich (Fluka no. 06668).

(25) Heersche, H. B.; de Groot, Z.; Folk, J. A.; van der Zant, H. S. J.; Romeike, C.; Wegewijs, M. R.; Zobbi, L.; Barreca, D.; Tondello, E.; Cornia, A. *Phys. Rev. Lett.* **2006**, *96*, 206801.

(26) Jo, M.-H.; Grose, J. E.; Baheti, K.; Deshmukh, M. M.; Sokol, J. J.; Rumberger, E. M.; Hendrickson, D. N.; Long, J. R.; Park, H.; Ralph, D. C. *Nano Lett.* **2006**, *6*, 2014.

NL062631I